LIQUID CRYSTALS, 1994, VOL. 17, NO. 2, 243–261

Properties of higher-ordered ferroelectric liquid crystal phases of a homologous series

by I. DIERKING†, F. GIEßELMANN†, J. KUßEROW‡
and P. ZUGENMAIER*†

† Institut für Physikalische Chemie, TU Clausthal,
Arnold-Sommerfeld-Str. 4, D-38678 Clausthal-Zellerfeld, Germany
‡ Institut für Organische Chemie, TU Clausthal,
Leibnizstr. 6, D-38678 Clausthal-Zellerfeld, Germany

(*Received 23 August 1993; accepted 9 November 1993*)

Four members of a homologous series of diarylethane α-chloroester ferroelectric liquid crystals [1] have been synthesized and characterized by polarizing optical microscopy and DSC measurements. Two of the compounds exhibit a twist grain boundary structure (TGB A* phase) or twisted smectic A* phase, shortly before reaching the smectic to cholesteric phase transition. The temperature dependence of the optical tilt angle θ, the spontaneous polarization P_S and the effective rotational viscosity γ_φ were investigated for the ferroelectric S_C^*, S_I^* and S_F^* phases. It was found that especially the spontaneous polarization and the rotational viscosity increased with decreasing length of the alkyl chain for all three ferroelectric phases. At the phase transition from S_C^* to S_I^*, all material parameters determined showed a discontinuous change, giving evidence for a first order transition. At the transition from the S_I^* to the S_F^* phase, the material parameters show only small, rather continuous changes.

1. Introduction

Since the discovery of ferroelectric liquid crystalline materials by Meyer *et al.* [2], and the proposal of the SSFLC geometry by Clark and Lagerwall [3], ferroelectric smectic C* phases have attracted great interest in liquid crystal research, but few systematic experimental data are available on physical properties and material constants of higher-ordered ferroelectric smectic phases [4–10]. In this paper we present the results of measurements of the temperature dependence of the optical tilt angle θ, the spontaneous polarization P_S and the effective rotational viscosity γ_φ in three ferroelectric mesophases, namely the S_C^*, S_I^* and S_F^* phases, for four members of a homologous series ($n = 5$–8) of diarylethane α-chloroesters, derived from D-valine. We have synthesized two homologous series of compounds. Series **I** relates to esters derived from L-valine

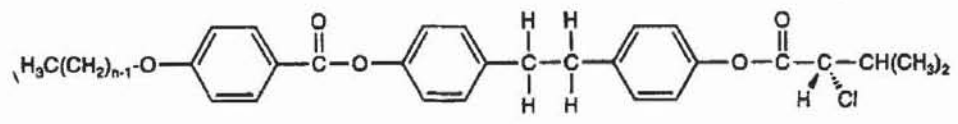

* Author for correspondence.

Nguyen *et al.* [1], have reported the synthesis, characterization and some electro-optical properties of series I ($n = 6$–12). Series **II** relates to the esters derived from D-valine

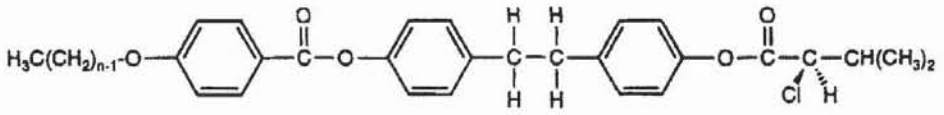

We report the synthesis, characterization and electro-optical properties of the $n = 5$–8 members of this new series.

The compounds of series **II** will be referred to as homologues D5, D6, D7 and D8 with $n = 5$, 6, 7 and 8, respectively; one of these compounds, D5, has been synthesized for the first time. The compounds of series **I** are code-lettered as L6–L12. A brief comment on the paper by Nguyen *et al.* [1] will be given, since results of some measurements on one compound of series **I** (n = 8, L8) show in part a large deviation from our results.

2. Experimental

The compounds of the homologous series **I** and **II** were synthesized according to the scheme. Details of the synthesis and the purification procedures are in § 5.

Polarizing optical microscopic studies were carried out with an Olympus BH-2 microscope equipped with a Mettler FP 52 hot stage. For texture observations, the samples were mounted on slides without surface alignment layers. All other measurements were performed by introducing the sample into commercially available liquid crystal cells (E.H.C. Co. Ltd.) with cell gap 4 μm. Calorimetric investigations were carried out with a differential scanning calorimeter (Perkin–Elmer DSC 7).

The temperature dependence of the spontaneous polarization was investigated using the triangular wave method [11]. The frequency of the applied electric field was 200 Hz for all measurements; the amplitude was varied between $E = 1$–$2\,\mathrm{MV\,m^{-1}}$ for the S_C^*, $E = 10$–$20\,\mathrm{MV\,m^{-1}}$ for the S_I^* and $E = 20$–$50\,\mathrm{MV\,m^{-1}}$ for the S_F^* phase, to assure saturated switching. Sixteen single measurements of the transient current were averaged to suppress statistical noise.

Electro-optic measurements, such as the determination of the switching time, were performed using an apparatus described elsewhere [12]. The experiments were carried out under the same conditions as those used for the determination of the spontaneous polarization, only applying a square wave field and averaging 64 single measurements. The switching time was defined as the change in the absolute transmission from 10–90 per cent. This response time was then used to estimate the effective rotational viscosity γ_φ using the relation [13]

$$\gamma_\varphi = \frac{1}{1{\cdot}8}\tau_{10\%-90\%} P_S E. \tag{1}$$

The optical tilt angle was measured by the method introduced by Bahr and Heppke [14] with the applied square wave electric field, amplitude and frequency mentioned above. While the sample is rotated between crossed polarizers, the intensity of the transmitted light of the stationary states varies as $\sin^2(2\varphi)$, with φ being the angle between the director and the polarization direction of one of the polarizers. For the determination of the optical tilt angle, the values of the transmitted light intensities of the two stationary states (polarization 'up' and 'down') were recorded by a

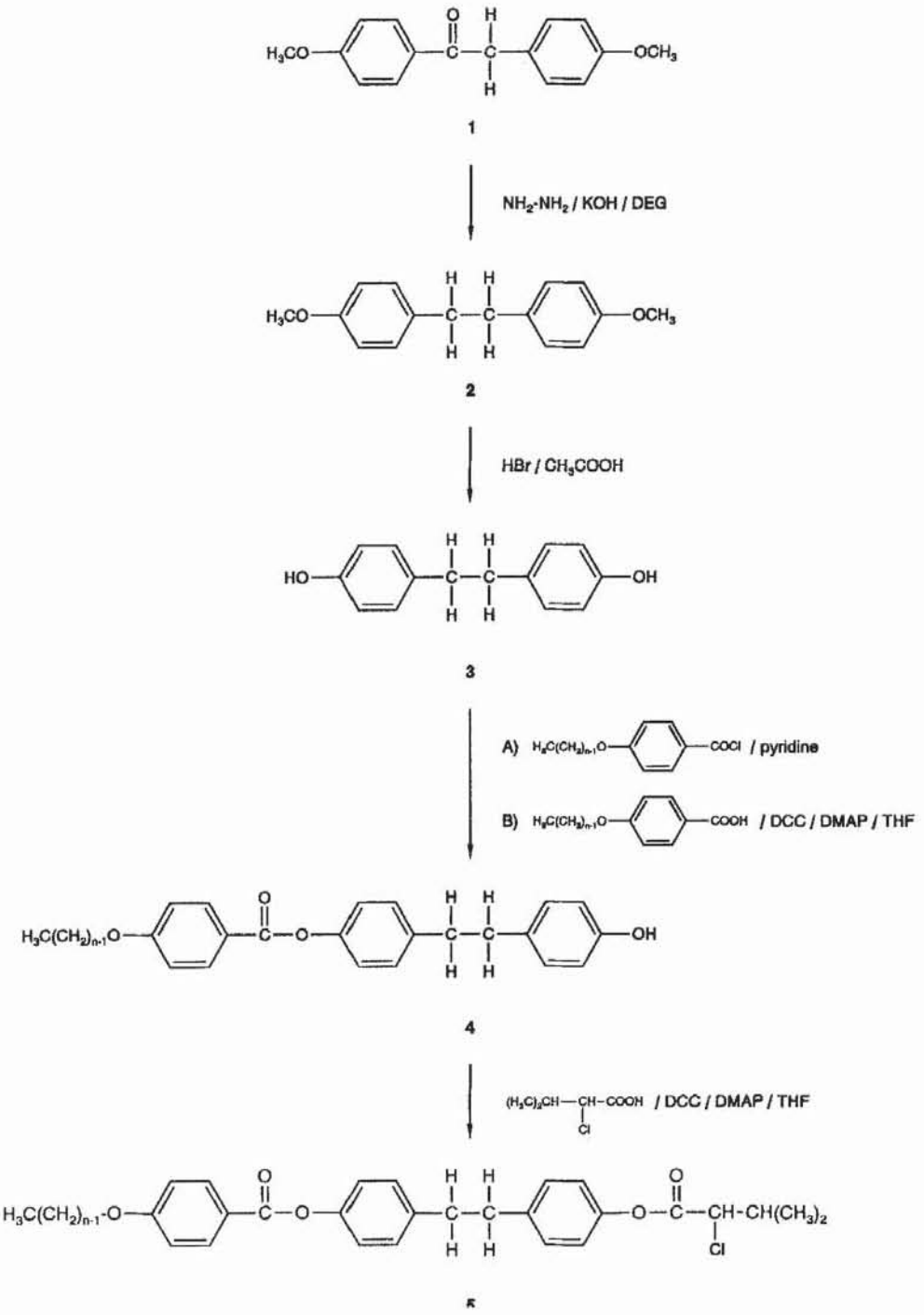

photomultiplier for several values of φ and then fitted with a simplex method according to relations (2*a*) and (2*b*)

$$I_{\text{up}} \sim \sin^2(2\varphi + \delta_{\text{up}}), \tag{2a}$$

$$I_{\text{down}} \sim \sin^2(2\varphi + \delta_{\text{down}}). \tag{2b}$$

The phase shift between the two curves for the intensities of the transmitted light for the polarization up and down states as a function of φ is then equal to twice the optical tilt angle

$$\delta_{\text{up}} - \delta_{\text{down}} = 2\theta. \tag{3}$$

X-ray investigations to determine the temperature dependence of the layer spacing d for compound D8 were performed with a Kratky small angle camera (Anton Paar KG), equipped with a position-sensitive counter (Firma M. Braun). Calibration with substances of known unit cell size and geometry leads to values for the layer spacings.

3. Experimental results and discussion

3.1. *Polarizing optical microscopy and DSC*

The compound D5 of the homologous series **II** was synthesized for the first time and the phase sequence on slowly cooling the sample from the isotropic phase in LC cells is given by

D5	I	134·1	N*	106·7	S_C^*	92·3	S_I^*	90·6 S_F^*
ΔH/kJ mol^{-1}		(2·1)		(0·4)		(2·4)		(0·2)

Numbers in brackets indicate the transition enthalpies ΔH in kJ mol^{-1} from DSC measurements (heating rate -5°C min^{-1}). The temperature control of the hot stage was within 0·1°C and the accuracy of absolute temperature values about ± 1°C. It should be noted, that all of the compounds investigated can be supercooled to about 30°C for several hours without crystallization

For compounds D7 and D8, a phase sequence was found which is slightly different from that reported in literature [1] for series **I**, as a TGB A* phase [15, 16] was detected over a small temperature interval of about 0·2°C by microscopy for both substances; this phase mediates the smectic A* to cholesteric transition (D8) and the smectic C* to cholesteric transition [17] (D7).

The notation S_A^* indicates a smectic A phase containing chiral molecules, which might be a non-helical smectic A phase or a TGB A* phase; the latter describes a helical smectic A phase (twist grain boundary phase). This notation follows the symmetry considerations discussed by Lagerwall [18].

Figures 1 (*a*)–(*f*) depict the mesomorphism of compound D8, observed by polarizing optical microscopy on cooling samples prepared on a glass slide without surface alignment layers. Figure 1 (*a*) shows a typical oily-streak texture of the cholesteric phase [19]. On further cooling the sample, the texture of a twist grain boundary phase TGB A* is observed [15, 16, 17] over a temperature interval of about 0·2°C (see figure 1 (*b*)) before the typical fan-shaped texture [19] of the chiral smectic A* phase is formed (see figure 1 (*c*)). Passing through the smectic A* to smectic C* transition, disclination lines appear across the fans, due to the helical director configuration of the S_C^* phase [20, 21] (see figure 1 (*d*)). This helical structure is partially maintained in the S_I^* phase (see figure 1 (*e*)) and in the S_F^* phase (see figure 1 (*f*)). The phase sequence for compound D8 on slowly cooling the sample in LC cells is

D8: I 134·5 N* 129·4 TGB A* 129·2 S_A^* 125·6 S_C^* 92·9 S_I^* 83·7 S_F^*.

The phase sequence for compound D7 is given by

D7: I 133·2 N* 121·1 TGB A* 120·8 S_C^* 92·4 S_I^* 86·1 S_F^*.

It should be noted that the transition temperatures obtained when using thin 4 μm liquid crystal cells are slightly different from the ones obtained by DSC, since the transition temperatures may depend on the sample thickness and preparation, a behaviour which has been observed for other compounds [21], and which is probably due to strong

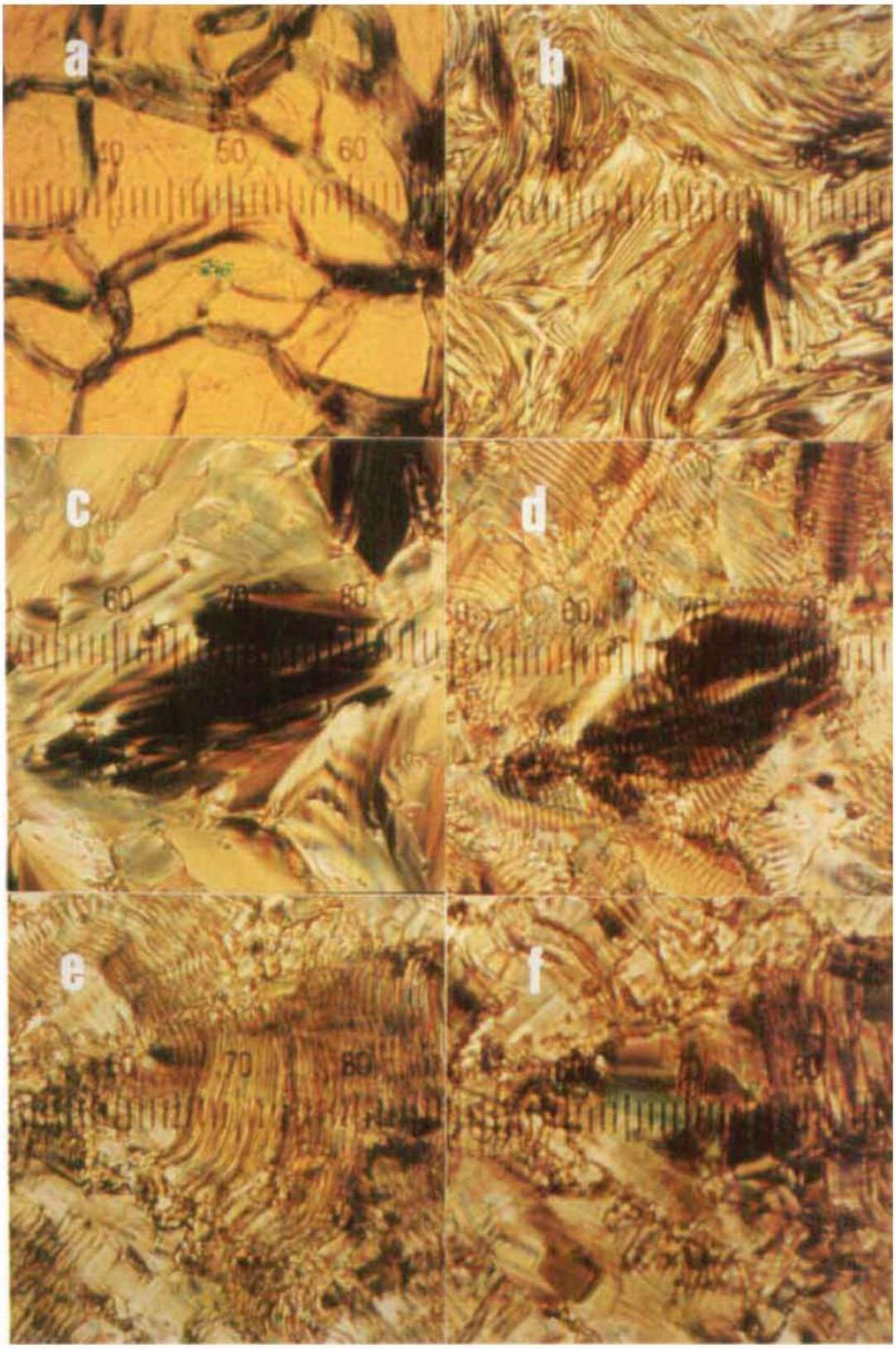

Figure 1. Typical polarizing optical microscopic textures of the mesophases of compound D8. (*a*) Cholesteric oily-streak texture ($T = 129{\cdot}5°C$), (*b*) texture of the twist grain boundary or TGB A* phase ($T = 129{\cdot}3°C$), (*c*) fan-shaped texture of the chiral smectic A (S_A^*) phase ($T = 128{\cdot}9°C$), (*d*) fan-shaped texture with disclination lines of the S_C^* phase ($T = 125{\cdot}6°C$), (*e*) S_I^* texture with disclination lines ($T = 92°C$) and (*f*) texture of the S_F^* phase. The sample was prepared on a glass slide with a cover slip without surface alignment layers. (10 units of scale $\triangleq 60\,\mu m$.)

surface effects in thin samples. Therefore, the temperature measured with thin cells are reported, since all experimental data below were measured using 4 μm LC cells.

For compound D6 the phase sequence is

D6: I 135·6 N* 114·6 S_C^* 90·5 S_I^* 87·2 S_F^*.

3.2. *The optical tilt angle*

The temperature dependence of the optical tilt angle for the three ferroelectric phases S_C^*, S_I^* and S_F^* for compounds D5, D6, D7 and D8 is depicted in figures 2 (*a*)–(*d*). Considering equal reduced temperatures with regard to the corresponding phase transitions, the measurements exhibit a slightly increasing optical tilt angle with

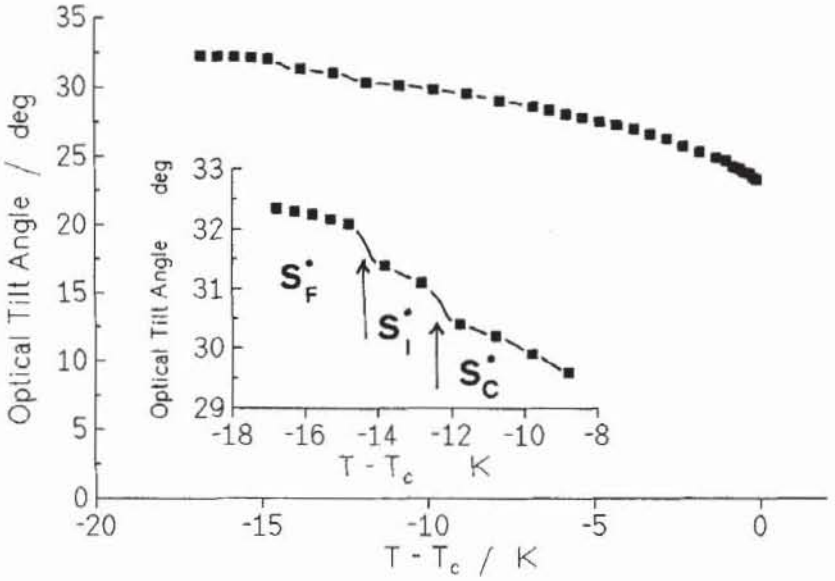

(*a*)

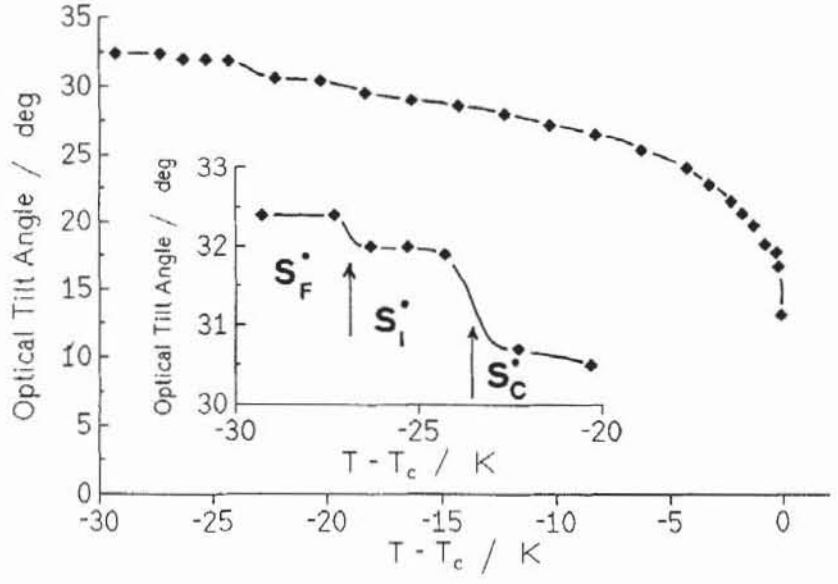

(*b*)

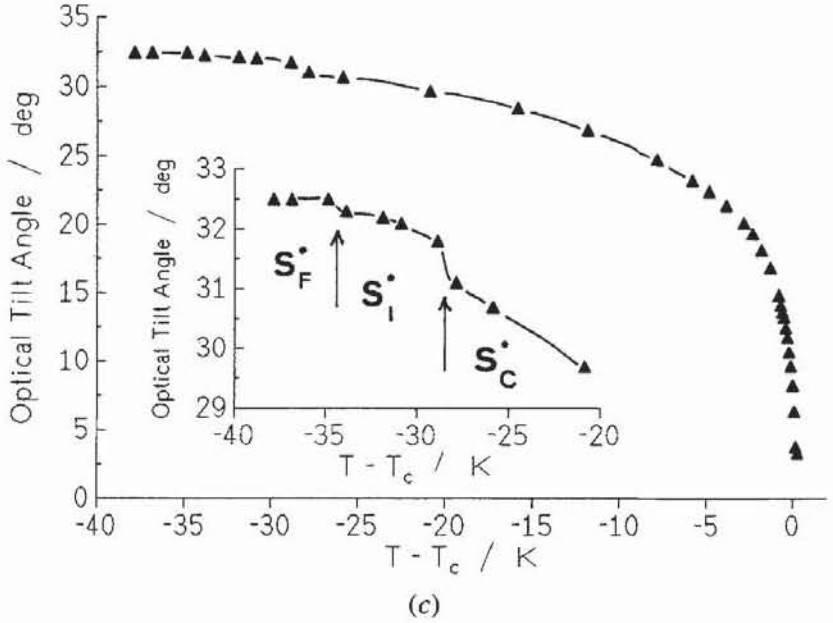

(*c*)

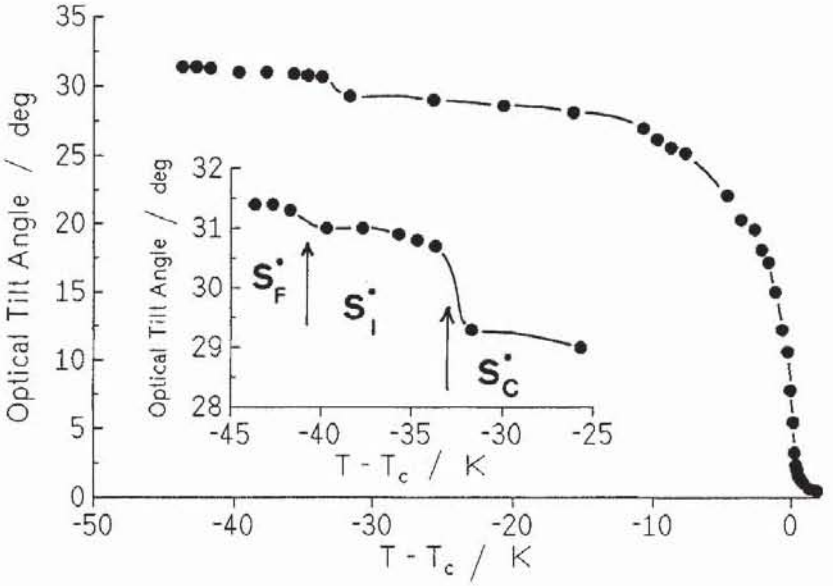

(*d*)

Figure 2. Temperature dependence of the optical tilt angle θ for the S_C^*, S_I^* and S_F^* phases for the compounds (*a*) D5, (*b*) D6, (*c*) D7 and (*d*) D8. The enlarged sections depict the respective phase transitions, indicated by arrows.

decreasing length of the alkyl chain in the S_C^* phase and, within experimental error, about equal optical tilt angles in the S_I^* and S_F^* phases.

For compounds D5 and D6 the optical tilt angle shows a steep discontinuous jump at the $N^* \rightarrow S_C^*$ transition, a behaviour which is commonly known for the first order $N^* \rightarrow S_C^*$ transition. Compounds D7 and D8 exhibit a more continuous change in tilt angle on passing the continuous $S_A^* \rightarrow S_C^*$ phase transition. The electroclinic effect in the S_A^* phase [22] of compound D8 is clearly detectable as depicted in figure 3. The induced optical tilt angle diverges on approaching the $S_A^* \rightarrow S_C^*$ phase transition, as is commonly observed. Passing the $S_C^* \rightarrow S_I^*$ phase transition, a discontinuous increase in

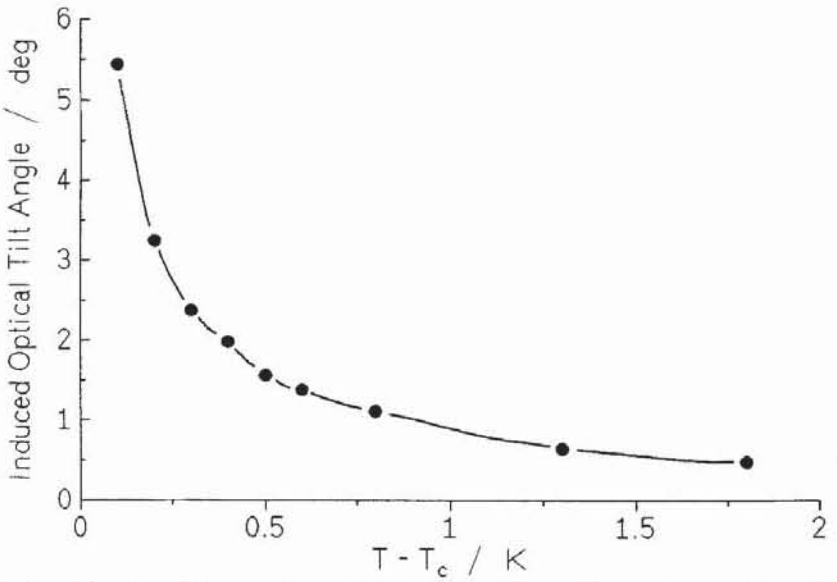

Figure 3. Induced optical tilt angle θ_{ind} as a function of the reduced temperature, demonstrating the electroclinic effect in the S_A^* phase of compound D8.

the optical tilt angle takes place, giving evidence for a first order transition (see enlarged plots in figure 2 (*a*)–(*d*)). The increase in optical tilt angle cannot be accounted for solely by the electroclinic effect [22] when the electric field is increased from 2 MV m^{-1} in the S_C^* phase to 10 MV m^{-1} in the S_I^* phase. Measurements made directly at the phase transition exhibit an increase in the optical tilt angle of only 0·3° with the large increase in the electric field strength. A smaller, but also slightly discontinuous increase in the tilt angle is also detected as the $S_I^* \rightarrow S_F^*$ transition is passed, probably due to the electroclinic effect.

3.3. *The spontaneous polarization*

The temperature dependence of the spontaneous polarization for the three ferroelectric smectic phases is depicted in figure 4. These measurements show a drastic deviation from results published for L8 by Nguyen *et al.* [1]. They found a sharply decreasing spontaneous polarization in the S_I^* and S_F^* phase as compared with the values for the S_C^* phase, whereas our measurements exhibit an increase in P_S with decreasing temperature for all three phases under investigation. This discrepancy may be due to an incomplete reorientation of the spontaneous polarization from $+P_S$ to $-P_S$. For a complete switching process in the S_I^* and S_F^* phase, the applied electric field E has to be increased to quite high amplitudes of 10–20 MV m^{-1} in the S_I^* and 20–50 MV m^{-1} in the S_F^* phase. The frequency of E should not be larger than 300 Hz.

Since the spontaneous polarization is coupled to the tilt angle, and the tilt angle increases with decreasing temperature over all three ferroelectric mesomorphic phases (see figure 2 (*a*)–(*d*)), the values obtained are most reasonable. A similar temperature behaviour of P_S, at least for the $S_C^* \rightarrow S_I^*$ transition, was also found by other authors for a different compound [5]. To confirm our results further, we performed small angle X-ray measurements to determine the layer spacing in all three ferroelectric smectic phases of compound D8. The values are depicted in figure 5. Within experimental error, the layer spacing stays constant at 30·7 Å all through the temperature ranges for the smectic I* and the smectic F* phases; this value is the same as that found by Nguyen *et al.* [1].

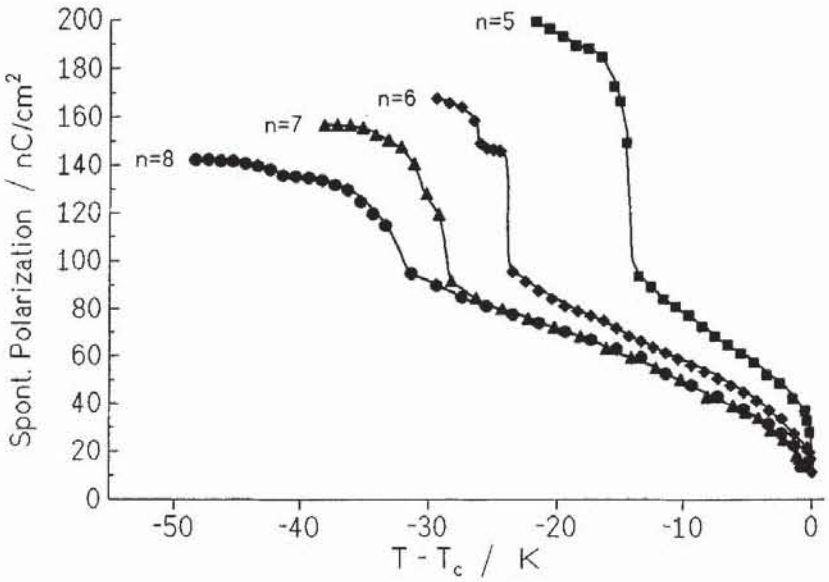

Figure 4. Temperature dependence of the spontaneous polarization P_S of the three ferroelectric mesophases S_C^*, S_I^* and S_F^* for compounds D5–D8. The phase transitions are clearly visible, illustrated by the discontinuous changes in P_S.

As can be seen in figures 4 and 6, the spontaneous polarization increases with decreasing length of the alkyl chain in all three ferroelectric mesophases at comparable reduced temperatures. This is the opposite behaviour of that usually found [23, 24]; one would rather expect the spontaneous polarization to increase with increasing alkyl chain length, which usually hinders the molecular rotation around the molecular long axis, thus increasing P_S [23, 24].

All members of the homologous series considered, exhibit a steep, discontinuous increase in the spontaneous polarization when passing the $S_C^* \rightarrow S_I^*$ phase transition, which is due to the coupling between the tilt angle (primary order parameter) and the spontaneous polarization and indicates that the transition is of first order. The height of the jump increases with decreasing length of the alkyl chain. Further evidence, that the transition from smectic C* to smectic I* is of first order, can be demonstrated by detecting the polarization reversal current while passing through the phase transition, as depicted in figures 7 (*b*)–(*f*) for compound D8. The applied electric field is depicted in figure 7 (*a*). Starting in the S_C^* phase at temperature $T = 94°C$ (see figure 7 (*b*)) and decreasing the temperature, one observes a second current peak evolving (see figures 7 (*c*)–(*e*), $T = 93{\cdot}25°C$, $93{\cdot}15°C$ and $93{\cdot}1°C$, respectively), which arises from the spontaneous polarization of the S_I^* phase, while the current peak resulting from the spontaneous polarization of the S_C^* phase diminishes until only the reversal current or polarization reorientation of the S_I^* phase is detected (see figure 7 (*f*), $T = 92°C$). For a second order phase transition, a continuous shift of the current peak along the time-scale would be expected, rather than a discontinuous evolution of the second peak while passing through the phase transition.

3.4. *The effective rotational viscosity*

The effective rotational viscosities were estimated by measuring the switching time as a function of temperature and evaluating equation (1). In all three ferroelectric mesophases, an increase in the viscosity is observed with decreasing length of the alkyl chain (see figures 8 (*a*)–(*c*)). This variation of the effective rotational viscosity with

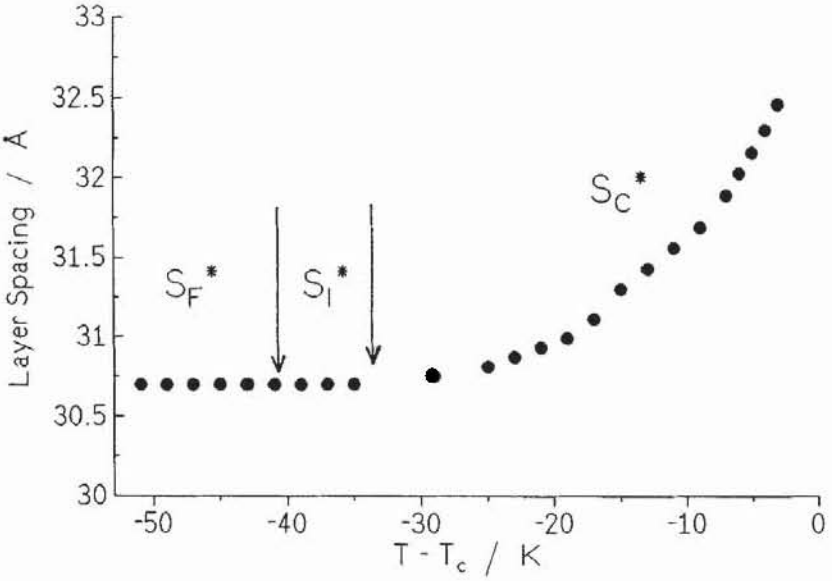

Figure 5. Temperature dependence of the layer spacing d of compound D8 for all three ferroelectric mesophases S_C^*, S_I^* and S_F^*.

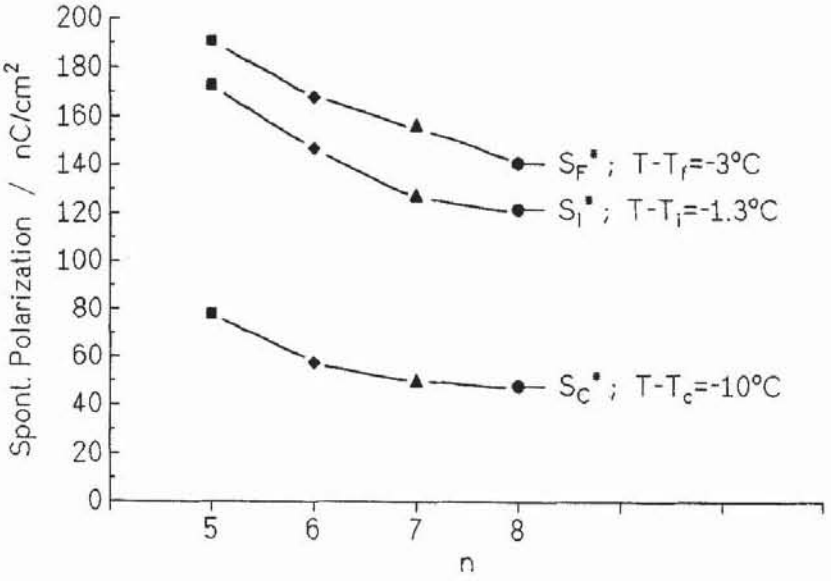

Figure 6. Variation of the spontaneous polarization P_S as a function of the number n of carbons in the alkyl chain for the ferroelectric S_C^*, S_I^* and S_F^* phases. An increase in P_S with decreasing length of the alkyl chain is observed for all three ferroelectric phases. The values are depicted for reduced temperatures T_c, T_i and T_f for the respective phase transitions.

chain length was also observed by Krishna Prasad *et al.* [25], for the S_C^* phase. A few degrees (about 5°C below the phase transition) into the smectic C* phase, an almost linear dependence of the viscosity on temperature is observed, while further away from the transition, the behaviour is Arrhenius-like (see figure 8 (*a*)). The kind of behaviour is often found for different compounds and mixtures [26]. In the S_C^* phase an increase in the activation energy E_A with decreasing chain length is found by a best-fit procedure, with $E_A = 183$, 105, 53 and 49 kJ mol^{-1} for compounds D5, D6, D7 and D8,

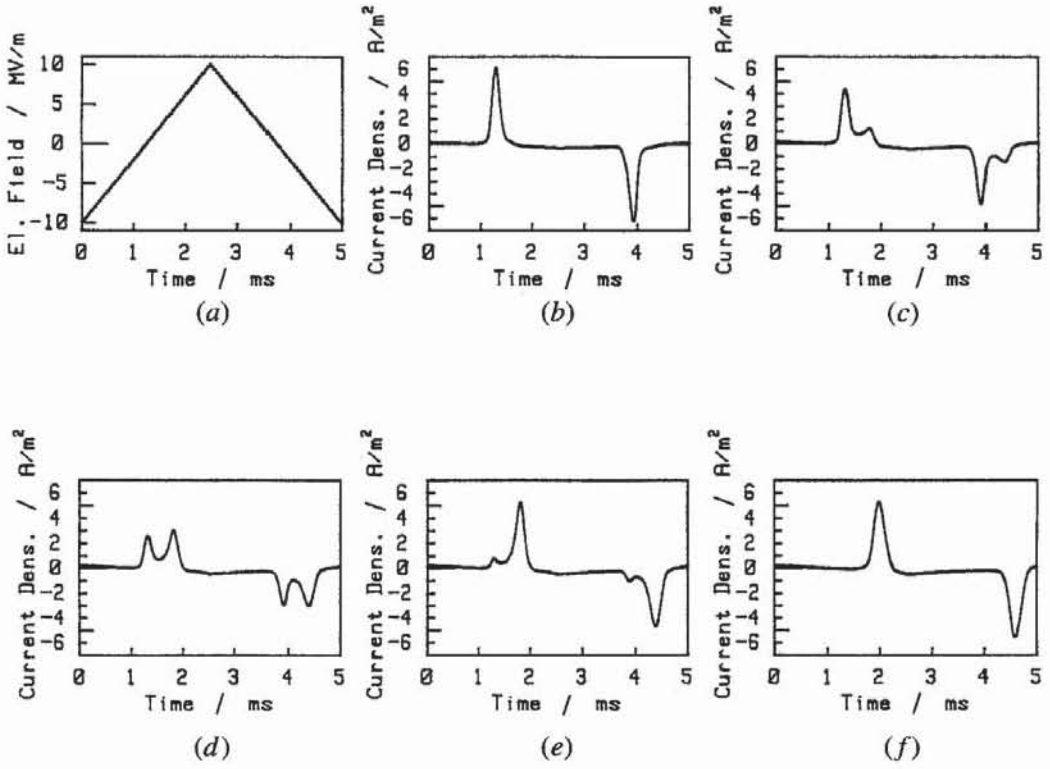

Figure 7. Polarization reversal current, on passing through the $S_C^* \rightarrow S_I^*$ phase transition. (*a*) Applied electric field, (*b*) S_C^* phase at $T = 94°C$, (*c*) $T = 93{\cdot}25°C$, (*d*) $T = 93{\cdot}15°C$, (*e*) 93·1°C and (*f*) S_I^* phase at $T = 92°C$.

respectively. Activation energies and values for the effective rotational viscosities of the S_C^* phase are of the order of magnitude obtained for other compounds [25, 27, 28].

Passing through the $S_C^* \rightarrow S_I^*$ phase transition, the viscosity strongly increases by about an order of magnitude and exhibits a linear temperature dependence in the S_I^* phase (see figure 8 (*b*)). This inverse proportional relationship between effective rotational viscosity and temperature is also found for the S_F^* phase (see figure 8 (*c*)).

4. Conclusions

In contrast to literature reports on diarylethane α-chloroesters derived from L-valine [1], we have detected a TGB A* state in some of the compounds of the D-series under investigation [17]. Compound D5 was synthesized for the first time and characterized by polarizing optical microscopy and DSC measurements.

Contrary to previously published data for the spontaneous polarization [1], systematic measurements of the temperature dependence of the optical tilt angle, the spontaneous polarization and the effective rotational viscosity in the S_C^*, S_I^* and S_F^* phases were found to increase with decreasing temperature, as is commonly known for the S_C^* phase.

The spontaneous polarization and the effective rotational viscosity increase in all three ferroelectric mesophases investigated with decreasing length of the alkyl chain, a behaviour which, at least for the spontaneous polarization, is unexpected [23, 24].

Experimental data obtained by different methods—DSC, microscopy, electric and electro-optic studies—indicate that the $S_C^* \rightarrow S_I^*$ phase transition is of first order, since all measured quantities exhibited a discontinuous change at the transition. Small

discontinuities in the physical parameters can be detected at the $S_I^* \rightarrow S_F^*$ transition, but are within experimental error and no definite conclusion concerning the order of this transition can be reached.

5. Experimental

5.1. *Analysis*

Melting points were determined using an electrical BÜCHI apparatus, model 520. ^{1}H NMR spectra were recorded using a BRUCKER ARX 400 (400 MHz), a Varian XL 200 (200 MHz) or a Varian A60-A (60 MHz) spectrometer using TMS as internal standard and deuterochloroform as solvent. Liquid chromatography was carried out on silica gel 60 (Merck, 0·063–0·200 mm) with dichloromethane as eluent.

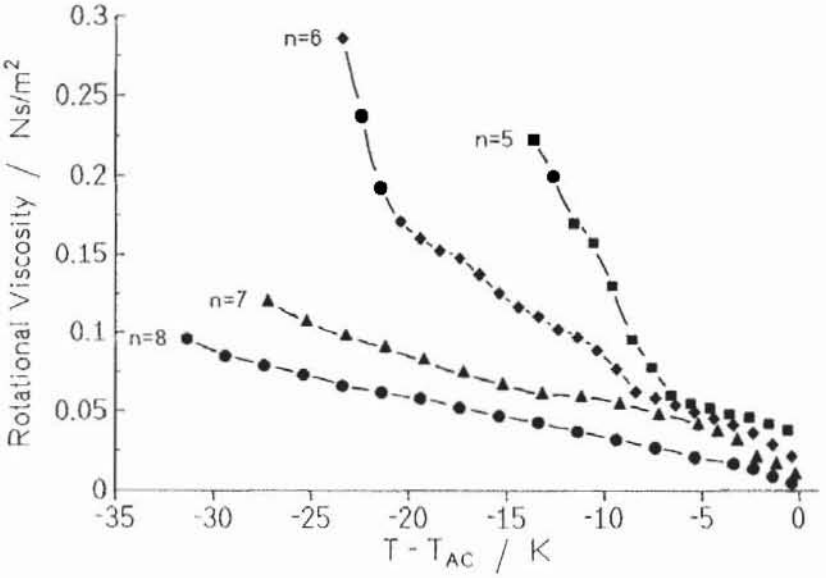

(*a*)

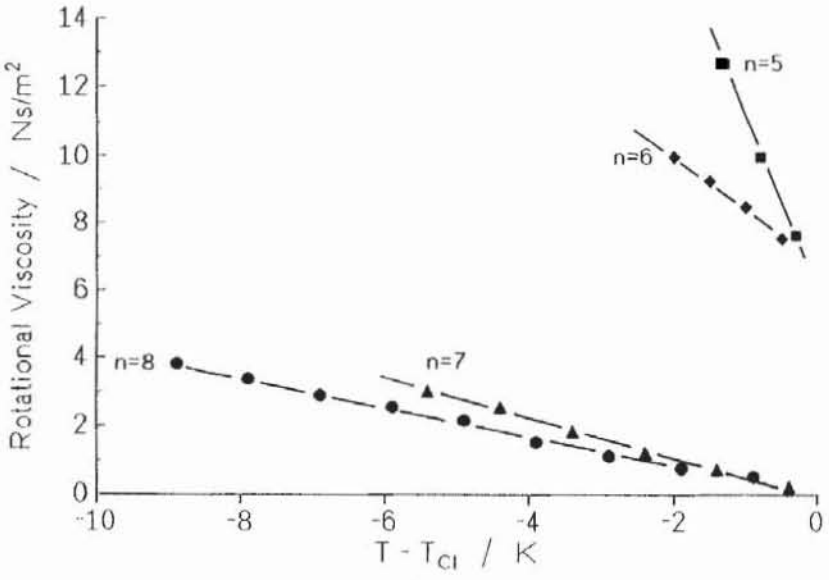

(*b*)

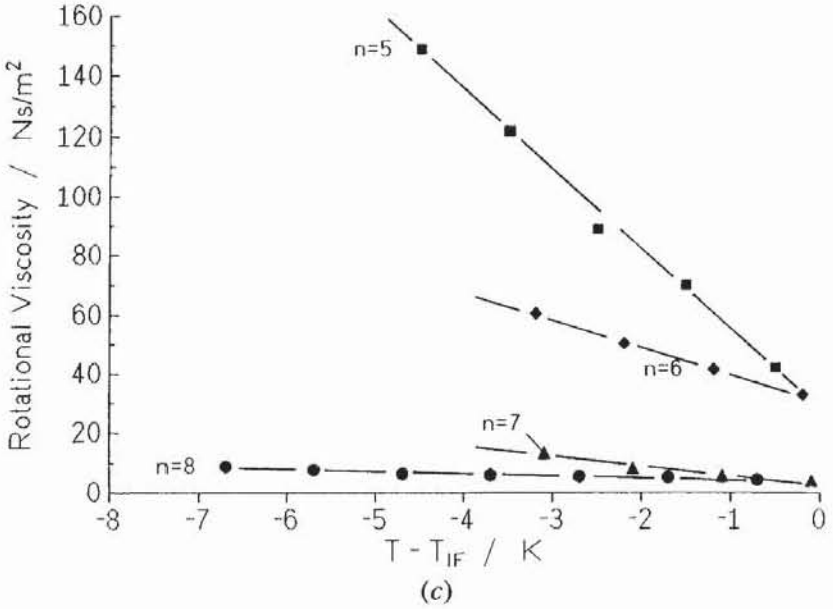

Figure 8. Temperature dependence of the effective rotational viscosity γ_φ for the compounds D5–D8 in the (*a*) S_C^*, (*b*) S_I^* and (*c*) S_F^* phases. The effective rotational viscosities increase with decreasing length of the alkyl chain al all three ferroelectric phases.

5.2. *Synthesis of 1,2-di(4-methoxyphenyl)ethane* (**2**)

A solution of 25·60 g (0·1 mol) of desoxy-4-anisoin (**1**) and 15 ml (0·3 mol) of 100 per cent hydrazine hydrate in 180 ml of triethylene glycol was heated under reflux for 20 min. After cooling to 40°C, 22 g (0·4 mol) of powdered KOH was added to the solution. The mixture was heated gradually to 200–210°C and maintained at this temperature until the evolution of nitrogen had ceased (4–5 h). The cooled mixture was hydrolysed with 2000 ml water and the organic material was extracted into dichloromethane (4 × 200 ml). The combined organic extracts were washed with 10 per cent hydrochloric acid (100 ml), water (3 × 100 ml) and dried over anhydrous Na_2SO_4. The solvent was evaporated and the product purified by chromatography and recrystallization from ethanol. Yield 22·51 g (93 per cent), m.p. = 127°C ([29] m.p. = 125·5–127°C).

5.3. *Synthesis of 1,2-di(4-hydroxyphenyl)ethane* (**3**)

After Richardson and Reid [29], a mixture of 24·23 g (0·1 mol) of **2** in 150 ml of glacial acetic acid and 40 ml of hydrobromic acid (48 per cent) was heated under reflux for 72 h. The cooled solution was added to 2000 ml water. The product was filtered off, washed with water (4 × 200 ml) and dried in vacuum. Yield 20·78 g (97 per cent, [29] 95 per cent), m.p. = 195–197°C ([29] m.p. = 198–199°C).

5.4. *General procedure for the reaction of 1,2-di(4-hydroxyphenyl)ethane* (**3**) *with 4-alkyoxybenzoyl chlorides to give 4-[β-(4-hydroxyphenyl)ethyl]phenyl 4-alkoxybenzoates* (**4**)

4·82 g (0·02 mol) of **3** were dissolved in 200 ml of dry pyridine and cooled to 0°C. A solution of 0·02 mol of 4-alkoxybenzoyl chloride (obtained from the 4-alkyloxybenzoic acid and an excess of thionyl chloride) in 50 ml dry pyridine was added dropwise to the solution of **3** with vigorous stirring. The mixture was stirred

over-night at 0°C, and the solvent was evaporated in vacuum. The residual solid was hydrolysed with 10 ml of concentrated hydrochloric acid and 500 ml water. The solid was filtered off, washed with water (4 × 200 ml) and dried in vacuum. Purification by chromatography on silica gel with dichloromethane as eluent and recrystallization from dichloromethane gave **4a–4c**.

5.4.1. *4-[β-4-hydroxyphenyl)ethyl]phenyl 4-pentyloxybenzoate* (**4a**)

Yield 2·51 g (31 per cent); transition temperatures (°C): C 135·8 N 149·9 I. IR (KBr): ν (cm^{-1}) = 3400, 1720, 1600, 1500, 1290, 1250. ^1H NMR (200 MHz): δ = 0·94 (t, J = 7 Hz, 3 H, $O(CH_2)_4CH_3$), 1·30–1·57 (m, 4 H, $OCH_2CH_2CH_2CH_2CH_3$), 1·72–1·92 (m, 2 H, $OCH_2CH_2CH_2CH_2CH_3$), 2·86 (s, 4 H, $2CH_2Ar$), 4·04 (t, J = 7 Hz, 2 H, $OCH_2CH_2CH_2CH_2CH_3$), 4·76 (s, 1 H, OH), 6·74 (d, J = 8 Hz, Ar), 6·94–7·24 (m, 8 H, Ar), 8·13 (d, J = 8 Hz, 2 H, Ar). Analysis: calculated for $C_{26}H_{28}O_4$ (405·5): C 77·20, H 6·98, O 15·82; found: C 77·60, H 6·90, O 15·53.

5.4.2. *4-[β-(4-hydroxyphenyl)ethyl]phenyl 4-hexyloxybenzoate* (**4b**)

Yield 0·50 g (6 per cent); transition temperatures (°C): C 137·8 N 148·6 I ([1] C 130 N 152 I). IR (KBr): ν (cm^{-1}) = 3400, 1715, 1600, 1500, 1290, 1240. ^1H NMR (200 MHz): δ = 0·91 (t, J = 7 Hz, 3 H, $O(CH_2)_5CH_3$), 1·22–1·66 (m, 6 H, $OCH_2CH_2(CH_2)_3CH_3$), 1·83 (quint, J = 7 Hz, 2 H, $OCH_2CH_2(CH_2)_3CH_3$), 2·89 (s, 4 H, $2CH_2Ar$), 4·06 (t, J = 6 Hz, 2 H, $OCH_2(CH_2)_4CH_3$), 4·77 (s, 1 H, OH), 6·75 (d, J = 8 Hz, 2 H, Ar), 6·91–7·31 (m, 8 H, Ar), 8·16 (d, J = 8 Hz, 2 H, Ar). Analysis: calculated for $C_{27}H_{30}O_4$ (418·5): C 77·48, H 7·23, O 15·29; found: C 77·52, H 7·20, O 15·25.

5.4.3. *4-[β-(4-hydroxyphenyl)ethyl]phenyl 4-heptyloxybenzoate* (**4c**)

Yield 2·34 g (27 per cent); transition temperatures (°C) C 135 N 143 I ([1] C 134 N 146 I). IR (KBr): ν (cm^{-1}) = 3400, 1715, 1600, 1500, 1290, 1250. ^1H NMR (200 MHz): δ = 0·82–0·94 (m, 3 H, $O(CH_2)_6CH_3$), 1·18–1·54 (m, 8 H, $OCH_2CH_2(CH_2)_4CH_3$), 1·70–1·89 (m, 2 H, $OCH_2CH_2(CH_2)_4CH_3$), 2·85 (s, 4 H, $2CH_2Ar$), 4·02 (t, J = 7 Hz, 2 H, $OCH_2(CH_2)_5CH_3$), 4·75 (s, 1 H, OH), 6·72 (d, J = 8 Hz, 2 H, Ar), 6·91–7·22 (m, 8 H, Ar), 8·13 (d, J = 8 Hz, 2 H, Ar). Analysis: calculated for $C_{28}H_{32}O_4$ (432·6): C 77·75, H 7·46, O 14·79; found: C 77·72, H 7·53, O 14·96.

5.5. *General procedure for the reaction of 1,2-di(hydroxyphenyl)ethane* (**3**) with *4-alkoxybenzoic acids to 4-[β-(4-hydroxyphenyl)ethyl]phenyl 4-alkoxybenzoates* (**4**)

A solution of 2·14 g (0·01 mol) of **3**, 0·01 mol of benzoic acid, 2·47 g (0·012 mol) of dicyclohexylcarbodiimide (DCC) and 40 mg of 4-(dimethylamino)pyridine (DMAP) in 20 ml of dry THF was stirred overnight at 0°C. The solvent was evaporated in vacuum and the residue purified by chromatography on silica gel with dichloromethane as eluent and by recrystallization from dichloromethane.

5.5.1. *4-[β-(4-hydroxyphenyl)ethyl]phenyl 4-octyloxybenzoate* (**4d**)

Yield 1·25 g (28 per cent); transition temperatures (°C): C 137·7 N 144·3 I ([1] C 131 N 144 I). IR (KBr): ν (cm^{-1}) = 3400, 1720, 1600, 1500, 1290, 1240. ^1H NMR (200 MHz): δ = 0·80–0·92 (m, 3 H, $O(CH_2)_7CH_3$), 1·18–1·52 (m, 10 H, $OCH_2CH_2(CH_2)_5CH_3$), 1·70–1·89 (m, 2 H, $OCH_2CH_2(CH_2)_5CH_3$), 2·85 (s, 4 H, $2CH_2Ar$), 4·01 (t, J = 7 Hz, 2 H, $OCH_2(CH_2)_6CH_3$), 4·73 (s, 1 H, OH), 6·72 (d, J = 8 Hz,

2 H, Ar), 6·90–7·26 (m, 8 H, Ar), 8·12 (d, $J = 8$ Hz, 2 H, Ar). Analysis: calculated for $C_{29}H_{34}O_4$ (446·6): C 78·00, H 7·67, O 14·33; found: C 78·17, H 7·71, O 14·53.

5.5.2. *4-[β-(4-hydroxyphenyl)ethyl]phenyl 4-nonyloxybenzoate* (**4e**)

Yield 3·09 g (67 per cent); transition temperatures (°C): C 136·1 N 141·1 I ([1] C 134 N 142 I). IR (KBr): ν (cm^{-1}) = 3400, 1720, 1600, 1500, 1290, 1250. ^1H NMR (200 MHz): $\delta = 0{\cdot}79$–$0{\cdot}93$ (m, 3 H, $O(CH_2)_8CH_3$), 1·17–1·51 (m, 12 H, $OCH_2CH_2(CH_2)_6CH_3$), 1·79 (quint, $J = 7$ Hz, 2 H, $OCH_2CH_2(CH_2)_6CH_3$), 2·86 (s, 4 H, $2CH_2Ar$), 4·02 (t, $J = 7$ Hz, 2 H, $OCH_2(CH_2)_7CH_3$), 4·76 (s, 1 H, OH), 6·73 (d, $J = 8$ Hz, 2 H, Ar), 6·90–7·23 (m, 8 H, Ar), 8·11 (d, $J = 8$ Hz, 2 H, Ar). Analysis: calculated for $C_{30}H_{36}O_4$ (460·6): C 78·23, H 7·88, O 13·89; found: C 78·22, H 7·79, O 13·98.

5.6. *4-Alkoxybenzoic acids*

The 4-alkoxybenzoic acids were synthesized according to [30–33].

5.7. *2-Chloro-3-methylbutanoic acids*

The chiral amino acids (L)-valine and (D)-valine were transformed to the corresponding (*S*)- and (*R*)-*2-chloro-3-methylbutanoic* acids, respectively, according to the method of Fu *et al.* [34].

5.8. *(S)-2-chloro-3-methylbutanoic acids from (L)-valine*

Yield 13·89 g (51 per cent), b.p. 98–102°C/16 hPa, n_D^{20} 1·4429.

5.9. *(R)-2-chloro-3-methylbutanoic acids from (D)-valine*

Yield 9·93 g (36 per cent), b.p. 98°C/14 hPa, n_D^{20} 1·4431.

5.10. *General procedure for the reaction of 4-[β-(4-hydroxyphenyl]ethyl]phenyl 4-alkoxybenzoates* (**4**) *with 2-chloro-3-methylbutanoic acids to yield 4-[β-{4-(2-chloro-3-methylbutanoyloxy)phenyl}-ethyl]phenyl 4-alkoxybenzoates* (**5**)

A solution of 0·002 mol of **4**, 0·287 g (0·0021 mol) of *2-chloro-3-methylbutanoic acid*, 0·473 g (0·0023 mol) of DCC and 20 mg of DMAP in 20 ml of dry THF was stirred overnight at 0°C. The precipitate was filtered off and washed three times with 10 ml of dry THF. The solvent was evaporated off, and the solid was chromatographed on silica gel with dichloromethane as eluent. After recrystallization from ethanol, the desired product was stirred overnight in 500 ml of distilled water. The product was filtered off and recrystallized from ethanol.

5.10.1. *4-[β-{4-{(S)-2-chloro-3-methylbutanoyloxy}phenyl}ethyl]phenyl 4-pentyloxybenzoate* (**5S1**)

Yield 754 mg (72 per cent). IR (KBr): ν (cm^{-1}) = 2960–2840, 1750, 1720, 1600, 1500, 1255, 1190, 1155. ^1H NMR (400 MHz): $\delta = 0{\cdot}947$ (t, $J = 7{\cdot}12$ Hz, 3 H, $O(CH_2)_4CH_3$), 1·151 (d, $J = 6{\cdot}64$ Hz, 6 H, $CH(CH_3)_2$), 1·35–1·51 (m, 4 H, $OCH_2CH_2CH_2CH_2CH_3$), 1·830 (quint, $J = 6{\cdot}99$ Hz, 2 H, $OCH_2CH_2CH_2CH_2CH_3$), 2·465, (o, $J = 6{\cdot}68$ Hz, 1 H, $CH(CH_3)_2$), 2·931 (s, 4 H, $2CH_2Ar$), 4·042 (t, $J = 6{\cdot}48$ Hz, 2 H, $OCH_2(CH_2)_3CH_3$), 4·326 (d, $J = 6{\cdot}60$ Hz, 1 H, CHCl), 6·965 (d, $J = 8{\cdot}64$ Hz, 2 H, Ar), 7·028 (d, $J = 8{\cdot}64$ Hz, 2 H, Ar), 7·107 (d, $J = 8{\cdot}68$ Hz, 2 H, Ar), 7·199 (d, $J = 8{\cdot}64$ Hz, 4 H, Ar), 8·134 (d, $J = 8{\cdot}64$ Hz, 2 H, Ar).

5.10.2. *4-[β-{4-{(R)-2-chloro-3-methylbutanoyloxy}phenyl}ethyl]phenyl 4-pentyloxybenzoate* (**5R1**)

Yield 779 mg (75 per cent). IR (KBr): ν (cm^{-1}) = 2950–2840, 1750, 1720, 1600, 1500, 1255, 1190, 1155, 1065. ^{1}H NMR (400 MHz): δ = 0·947 (t, J = 7·12 Hz, 3 H, $O(CH_2)_4CH_3$), 1·152 (d, J = 6·61 Hz, 6 H, $CH(CH_3)_2$), 1·35–1·51 (m, 4 H, $OCH_2CH_2CH_2CH_2CH_3$), 1·829 (quint, J = 6·99 Hz, 2 H, $OCH_2CH_2CH_2CH_2CH_3$), 2·464, (o, J = 6·68 Hz, 1 H, $CH(CH_3)_2$), 2·931 (s, 4 H, $2CH_2Ar$), 4·042 (t, J = 6·60 Hz, 2 H, $OCH_2(CH_2)_3CH_3$), 4·326 (d, J = 6·80 Hz, 1 H, CHCl), 6·965 (d, J = 9·20 Hz, 2 H, Ar), 7·029 (d, J = 8·04 Hz, 2 H, Ar), 7·107 (d, J = 8·80 Hz, 2 H, Ar), 7·199 (d, J = 7·20 Hz, 4 H, Ar), 8·133 (d, J = 8·65 Hz, 2 H, Ar). Analysis: calculated for $C_{31}H_{35}O_5Cl$ (523·07): C 71·18, H 6·74, O 15·29, Cl 6·78; found: C 71·12, H 6·78, O 15·37, Cl 6·73.

5.10.3. *4-[β-{4-{(S)-2-chloro-3-methylbutanoyloxy}phenyl}ethyl]phenyl 4-hexyloxybenzoate* (**5S2**)

Yield 776 mg (72 per cent). IR (KBr): ν (cm^{-1}) = 2960–2840, 1750, 1720, 1600, 1500, 1260, 1190, 1160. ^{1}H NMR (400 MHz): δ = 0·918 (t, J = 7·12 Hz, 3 H, $O(CH_2)_5CH_3$), 1·152 (d, J = 6·60 Hz, 6 H, $CH(CH_3)_2$), 1·28–1·41 (m, 4 H, $O(CH_2)_3CH_2CH_2CH_3$), 1·42–1·53 (m, 2 H, $OCH_2CH_2CH_2CH_2CH_2CH_3$),1·820 (quint, J = 6·99 Hz, 2 H, $OCH_2CH_2(CH_2)_3CH_3$), 2·466, (o, J = 6·68 Hz, 1 H, $CH(CH_3)_2$), 2·932 (s, 4 H, $2CH_2Ar$), 4·041 (t, J = 6·62 Hz, 2 H, $OCH_2(CH_2)_4CH_3$), 4·325 (d, J = 6·60 Hz, 1 H, CHCl), 6·965 (d, J = 9·16 Hz, 2 H, Ar), 7·029 (d, J = 8·12 Hz, 2 H, Ar), 7·107 (d, J = 8·64 Hz, 2 H, Ar), 7·199 (d, J = 7·12 Hz, 4 H, Ar), 8·134 (d, J = 8·68 Hz, 2 H, Ar).

5.10.4. *4-[β-{4-{(R)-2-chloro-3-methylbutanoyloxy}phenyl}ethyl]phenyl 4-hexyloxybenzoate* (**5R2**)

Yield 797 mg (74 per cent). IR (KBr): ν (cm^{-1}) = 2960–2840, 1750, 1720, 1600, 1500, 1255, 1190, 1170. ^{1}H NMR (400 MHz): δ = 0·917 (t, J = 6·86 Hz, 3 H, $O(CH_2)_5CH_3$), 1·151 (d, J = 6·64 Hz, 6 H, $CH(CH_3)_2$), 1·29–1·41 (m, 4 H, $OCH_2CH_2CH_2CH_2CH_2CH_3$), 1·43–1·53 (m, 2 H, $OCH_2CH_2CH_2CH_2CH_2CH_3$) 1·819 (quint, J = 6·99 Hz, 2 H, $OCH_2CH_2(CH_2)_3CH_3$), 2·464, (o, J = 6·71 Hz, 1 H, $CH(CH_3)_2$), 2·931 (s, 4 H, $2CH_2Ar$), 4·040 (t, J = 6·62 Hz, 2 H, $OCH_2(CH_2)_4CH_3$), 4·324 (d, J = 6·61 Hz, 1 H, CHCl), 6·966 (d, J = 9·15 Hz, 2 H, Ar), 7·028 (d, J = 8·65 Hz, 2 H, Ar), 7·106 (d, J = 8·13 Hz, 2 H, Ar), 7·197 (d, J = 8·14 Hz, 4 H, Ar), 8·134 (d, J = 9·16 Hz, 2 H, Ar). Analysis: calculated for $C_{32}H_{37}O_5Cl$ (537·09): C 71·56, H 6·94, O 14·89, Cl 6·60; found: C 71·66, H 7·09, O 14·58, Cl 6·67.

5.10.5. *4-[β-{4-{(S)-2-chloro-3-methylbutanoyloxy}phenyl}ethyl]phenyl 4-heptyloxybenzoate* (**5S3**)

Yield 796 mg (72 per cent). IR (KBr): ν (cm^{-1}) = 2950–2820, 1750, 1710, 1600, 1500, 1250, 1190, 1165. ^{1}H NMR (400 MHz): δ = 0·906 (t, J = 6·88 Hz, 3 H, $O(CH_2)_6CH_3$), 1·156 (d, J = 6·92 Hz, 6 H, $CH(CH_3)_2$), 1·28–1·53 (m, 8 H, $OCH_2CH_2(CH_2)_4CH_3$), 1·827 (quint, J = 7·01 Hz, 2 H, $OCH_2CH_2(CH_2)_4CH_3$), 2·469, (o, J = 6·69 Hz, 1 H, $CH(CH_3)_2$), 2·936 (s, 4 H, $2CH_2Ar$), 4·045 (t, J = 6·64 Hz, 2 H, $OCH_2(CH_2)_5CH_3$), 4·330 (d, J = 6·88 Hz, 1 H, CHCl), 6·969 (d, J = 8·88 Hz, 2 H, Ar), 7·033 (d, J = 8·84 Hz, 2 H, Ar), 7·111 (d, J = 8·36 Hz, 2 H, Ar), 7·203 (d, J = 7·40 Hz, 4 H, Ar), 8·138 (d, J = 8·88 Hz, 2 H, Ar).

5.10.6. *4-[β-{4-{(R)-2-chloro-3-methylbutanoyloxy}phenyl}ethyl]phenyl 4-heptyloxybenzoate* (**5R3**)

Yield 824 mg (75 per cent). IR (KBr): ν (cm^{-1}) = 2960–2840, 1745, 1720, 1595, 1500, 1250, 1190, 1160, 1060. ^1H NMR (400 MHz): δ = 0·902 (t, J = 6·88 Hz, 3 H, $O(CH_2)_6CH_3$), 1·152 (d, J = 6·60 Hz, 6 H, $CH(CH_3)_2$), 1·27–1·42 (m, 6 H, $OCH_2CH_2CH_2(CH_2)_3CH_3$), 1·43–1·52 (m, 2 H, $OCH_2CH_2CH_2(CH_2)_3CH_3$), 1·820 (quint, J = 7·12 Hz, 2 H, $OCH_2CH_2(CH_2)_4CH_3$), 2·465, (o, J = 6·68 Hz, 1 H, $CH(CH_3)_2$), 2·931 (s, 4 H, $2CH_2Ar$), 4·039 (t, J = 6·34 Hz, 2 H, $OCH_2(CH_2)_5CH_3$), 4·325 (d, J = 6·60 Hz, 1 H, CHCl), 6·964 (d, J = 8·64 Hz, 2 H, Ar), 7·028 (d, J = 8·16 Hz, 2 H, Ar), 7·107 (d, J = 8·64 Hz, 2 H, Ar), 7·197 (d, J = 8·68 Hz, 4 H, Ar), 8·134 (d, J = 8·64 Hz, 2 H, Ar). Analysis: calculated for $C_{33}H_{39}O_5Cl$ (551·12): C 71·92, H 7·13, O 14·51, Cl 6·27; found: C 72·38, H 7·47, O 13·81, Cl 6·34.

5.10.7. *4-[β-{4-{(S)-2-chloro-3-methylbutanoyloxy}phenyl}ethyl]phenyl 4-octyloxybenzoate* (**5S4**)

Yield 763 mg (68 per cent). IR (KBr): ν (cm^{-1}) = 2950–2840, 1755, 1715, 1600, 1500, 1250, 1190. ^1H NMR (400 MHz): δ = 0·894 (t, J = 6·88 Hz, 3 H, $O(CH_2)_7CH_3$), 1·151 (d, J = 6·60 Hz, 6 H, $CH(CH_3)_2$), 1·23–1·53 (m, 10 H, $OCH_2CH_2(CH_2)_5CH_3$), 1·819 (quint, J = 6·99 Hz, 2 H, $OCH_2CH_2(CH_2)_5CH_3$), 2·465, (o, J = 6·71 Hz, 1 H, $CH(CH_3)_2$), 2·930 (s, 4 H, $2CH_2Ar$), 4·038 (t, J = 6·62 Hz, 2 H, $OCH_2(CH_2)_6CH_3$), 4·327 (d, J = 6·60 Hz, 1 H, CHCl), 6·964 (d, J = 9·12 Hz, 2 H, Ar), 7·028 (d, J = 8·64 Hz, 2 H, Ar), 7·106 (d, J = 8·16 Hz, 2 H, Ar), 7·198 (d, J = 8·16 Hz, 4 H, Ar), 8·134 (d, J = 8·64 Hz, 2 H, Ar).

5.10.8. *4-[β-{4-{(R)-2-chloro-3-methylbutanoyloxy}phenyl}ethyl]phenyl 4-octyloxybenzoate* (**5R4**)

Yield 984 mg (87 per cent). IR (KBr): ν (cm^{-1}) = 2950–2840, 1755, 1720, 1600, 1500, 1250, 1190, ^1H NMR (400 MHz): δ = 0·900 (t, J = 6·66 Hz, 3 H, $O(CH_2)_7CH_3$), 1·157 (d, J = 6·88 Hz, 6 H, $CH(CH_3)_2$), 1·24–1·42 (m, 8 H, $OCH_2CH_2CH_2(CH_2)_4CH_3$), 1·43–1·54 (m, 2 H, $OCH_2CH_2CH_2$ $(CH_2)_4CH_3$), 1·825 (quint, J = 7·01 Hz, 2 H, $OCH_2CH_2(CH_2)_5CH_3$), 2·470, (o, J = 6·69 Hz, 1 H, $CH(CH_3)_2$), 2·936 (s, 4 H, $2CH_2Ar$), 4·044 (t, J = 6·64 Hz, 2 H, $OCH_2(CH_2)_6CH_3$), 4·331 (d, J = 6·88 Hz, 1 H, CHCl), 6·970 (d, J = 8·88 Hz, 2 H, Ar), 7·034 (d, J = 8·88 Hz, 2 H, Ar), 7·112 (d, J = 8·40 Hz, 2 H, Ar), 7·204 (d, J = 7·40 Hz, 4 H, Ar), 8·139 (d, J = 8·88 Hz, 2 H, Ar). Analysis: calculated for $C_{34}H_{41}O_5Cl$ (565·15): C 72·26, H 7·31, O 14·15, Cl 6·27; found: C 72·38, H 7·47, O 13·81, Cl 6·34.

5.10.9. *4-[β-{4-{(S)-2-chloro-3-methylbutanoyloxy}phenyl}ethyl]phenyl 4-nonyloxybenzoate* (**5S5**)

Yield 1085 mg (98 per cent). IR (KBr): ν (cm^{-1}) = 2940–2840, 1750, 1715, 1600, 1500, 1250, 1190, 1160. ^1H NMR (400 MHz): δ = 0·889 (t, J = 6·86 Hz, 3 H, $O(CH_2)_8CH_3$), 1·152 (d, J = 6·60 Hz, 6 H, $CH(CH_3)_2$), 1·22–1·53 (m, 12 H, $OCH_2CH_2(CH_2)_6CH_3$), 1·820 (quint, J = 6·99 Hz, 2 H, $OCH_2CH_2(CH_2)_6CH_3$), 2·466, (o, J = 6·68 Hz, 1 H, $CH(CH_3)_2$), 2·931 (s, 4 H, $2CH_2Ar$), 4·038 (t, J = 6·62 Hz, 2 H, $OCH_2(CH_2)_6CH_3$), 4·327 (d, J = 6·60 Hz, 1 H, CHCl), 6·965 (d, J = 9·12 Hz, 2 H, Ar), 7·029 (d, J = 8·64 Hz, 2 H, Ar), 7·104 (d, J = 10·50 Hz, 2 H, Ar), 7·200 (d, J = 7·12 Hz, 4 H, Ar), 8·134 (d, J = 9·16 Hz, 2 H, Ar).

5.10.10. *4-[β-{4-{(S)-2-chloro-3-methylbutanoyloxy}phenyl}ethyl]phenyl 4-nonyloxybenzoate* (**5S5**)

Yield 1023 mg (92 per cent). IR (KBr): ν (cm^{-1}) = 2905–2840, 1750, 1715, 1595, 1500, 1250, 1190, 1160. ^1H NMR (400 MHz): $\delta = 0{\cdot}888$ (t, $J = 6{\cdot}88$ Hz, 3 H, $O(CH_2)_8CH_3$), 1·152 (d, $J = 7{\cdot}12$ Hz, 6 H, $CH(CH_3)_2$), 1·22–1·41 (m, 10 H, $OCH_2CH_2CH_2(CH_2)_5CH_3$), 1·42–1·52 (m, 2 H, $OCH_2CH_2CH_2(CH_2)_5CH_3$), 1·818 (quint, $J = 7{\cdot}12$ Hz, 2 H, $OCH_2CH_2(CH_2)_6CH_3$), 2·465, (o, $J = 6{\cdot}68$ Hz, 1 H, $CH(CH_3)_2$), 2·931 (s, 4 H, $2CH_2Ar$), 4·039 (t, $J = 6{\cdot}60$ Hz, 2 H, $OCH_2(CH_2)_7CH_3$), 4·327 (d, $J = 6{\cdot}60$ Hz, 1 H, CHCl), 6·965 (d, $J = 8{\cdot}64$ Hz, 2 H, Ar), 7·028 (d, $J = 8{\cdot}64$ Hz, 2 H, Ar), 7·106 (d, $J = 8{\cdot}12$ Hz, 2 H, Ar), 7·199 (d, $J = 8{\cdot}64$ Hz, 4 H, Ar), 8·134 (d, $J = 8{\cdot}64$ Hz, 2 H, Ar). Analysis: calculated for $C_{35}H_{43}O_5Cl$ (579·17): C 72·58, H 7·48, O 13·81, Cl 6·12; found: C 72·63, H 7·60, O 13·69, Cl 6·08.

This work was supported by a grant from the Deutsche Forschungsgemeinschaft.

References

[1] Nguyen, H. T., Babeau, A., Léon, C., Marcerou, J.-P., Destrade, C., Soldera, A., Guillon, D., and Skoulios, A., 1991, *Liq. Crystals*, **9,** 253.
[2] Meyer, R. B., Liebert, L., Strzeleski, L., and Keller, P., 1975, *J. Phys. Lett., Paris*, **36,** L69.
[3] Clark, N. A., and Lagerwall, S. T., 1980, *Appl. Phys. Lett.*, **36,** 899.
[4] Goodby, J. W., Patel, J. S., and Leslie, T. M., 1984, *Ferroelectrics*, **59,** 121.
[5] Wahl, J., and Jain, S. C., 1984, *Ferroelectrics*, **59,** 161.
[6] Biradar, A. M., Wrobel, S., and Haase, W., 1989, *Ferroelectrics*, **99,** 149.
[7] Kuczynski, W., and Stegemeyer, H., 1989, *Liq. Crystals*, **5,** 553.
[8] Biradar, A. M., and Haase, W., 1990, *Liq. Crystals*, **7,** 143.
[9] Raja, V. N., Krishna Prasad, S., Shankar Rao, D. S., Goodby, J. W., and Neubert, M. E., 1991, *Ferroelectrics*, **121,** 235.
[10] Shao, R., Zhuang, Z., and Clark, N. A., 1991, *Ferroelectrics*, **122,** 213.
[11] Miyasato, K., Abe, S., Takezoe, H., Fukuda, A., and Kuze, E., 1983, *Jap. J. appl. Phys.*, **22,** L661.
[12] Gießelmann, F., and Zugenmaier, P., 1990, *Liq. Crystals*, **8,** 361.
[13] Kimura, S., Nishiyama, S., Ouchi, Y., Takezoe, H., and Fukuda, A., 1987, *Jap. J. appl. Phys.*, **26,** L255.
[14] Bahr, Ch., and Heppke, G., 1987, *Liq. Crystals*, **2,** 825.
[15] Goodby, J. W., Waugh, M. A., Stein, S. M., Chin, E., Pindak, R., and Patel, J. S., 1989, *Nature, Lond.*, **337,** 449.
[16] Goodby, J. W., Waugh, M. A., Stein, S. M., Chin, E., Pindak, R., and Patel, J. S., 1989, *J. Am. chem. Soc.*, **111,** 8119.
[17] Dierking, I., Gießelmann, F., and Zugenmaier, P., 1994, *Liq. Crystals*, **17,** 17.
[18] Lagerwall, S. T., 1988, *Ferroelectrics*, **85,** 497.
[19] Demus, D., and Richter, L., 1978, *Textures of Liquid Crystals* (Verlag Chemie, Weinheim).
[20] Martinot-Lagarde, Ph., 1976, *J. Phys., Paris, Colloque*, **37,** 129.
[21] Martinot-Lagarde, Ph., Duke, R., and Durand, G., 1981, *Molec. Crystals liq. Crystals*, **75,** 249.
[22] Garoff, S., and Meyer, R. B., 1977, *Phys. Rev. Lett.*, **38,** 848.
[23] Goodby, J. W., Patel, J. S., and Chin, E., 1987, *J. phys. Chem. Lett.*, **91,** 5151.
[24] Goodby, J. W., 1991, *Ferroelectric Liquid Crystals, Principles, Properties and Applications* (Gordon & Breach), p. 205.
[25] Krishna Prasad, S., Khened, S. M., Raja, V. N., and Shivkumar, B., 1991, *Ferroelectrics*, **121,** 319.
[26] Dierking, I., Gießelmann, F., and Zugenmaier, P. (unpublished results).
[27] Escher, C., Geelhaar, T., and Böhm, E., 1988, *Liq. Crystals*, **3,** 469.
[28] Escher, C., Dübal, H.-R., Hemmerling, W., Müller, I., Ohlendorf, D., and Wingen, R., 1988, *Ferroelectrics*, **84,** 89.

[29] RICHARDSON, E. M., and REID, E. E., 1940, *J. Am. chem. Soc.*, **62,** 413.
[30] BENNETT, G. M., and JONES, B., 1939, *J. chem. Soc.*, p. 420.
[31] GRAY, G. W., and JONES, B., 1953, *J. chem. Soc.*, p. 4179.
[32] JONES, B., 1935, *J. chem. Soc.*, p. 1874.
[33] NAIKWADI, K. P., JADHAV, A. L., SOUJ, R., and HATANO, H., 1986, *Makromolek. Chem.*, **187,** 1407.
[34] FU, S.-C. J., BIRNBAUM, S. M., and GRUNSTEIN, J. P., 1940, *J. Am. chem. Soc.*, **76,** 6054.